

Analysis of Stereochemical Convergence in Asymmetric Pd-Catalysed Allylic Alkylation Reactions Complicated by Halide and Memory Effects

Ian J. S. Fairlamb,^[a, b] Guy C. Lloyd-Jones,^{*[a]} Štěpán Vyskočil,^[c, d] and Pavel Kočovský^[c]

Abstract: A quantitative two-term description of memory effects arising in Pd-catalysed allylic alkylation reactions formally proceeding through 'meso'-type π -allylpalladium intermediates is presented. The utility of this description (stereochemical convergence (*sc*) and global enantiomeric excess (*ee_g*)) is demonstrated by application to a series of Pd-catalysed allylic alkylation reactions involving racemic cyclopentenyl esters. Analysis of such reactions, by employing a range of enantiomerically pure monophosphine ligands, reinforces the conclusion that selectivities (enantiomeric excess (*ee*) values) obtained under standard 'benchmark' type condi-

tions may be very misleading when powerful memory effects are operative. However, by comparison of *sc* and *ee* for a given ligand/solvent combination under a range of related conditions, one may predict the limiting ('latent') selectivity that will be obtained when the memory effect is negated. This technique is exemplified with one particular ligand (**4b**, 'MAP') for which a number of strategies were employed to find

conditions that negate the memory effect and reveal the limiting selectivity of the ligand. These conditions give a higher limiting global selectivity than that obtainable by using standard diastereoisomer equilibration methods such as added halide. Thus, the analysis of *sc* versus *ee_g* also allows subtle changes in selectivity to be discerned. The difference in limiting selectivity (chloride versus non-chloride conditions) is proposed to arise through the nucleophilic attack of neutral monodentate versus cationic bidentate MAP (**4b**) or MOP (**4a**) complexes.

Keywords: allylic compounds • asymmetric catalysis • memory effects • palladium • stereochemical convergence

Introduction

Over the last decade, asymmetric palladium-catalysed allylic alkylation^[1] has become a ubiquitous method for testing and comparing ('benchmarking') the efficacy of novel chiral ligands. Popular substrates for such reactions are those that

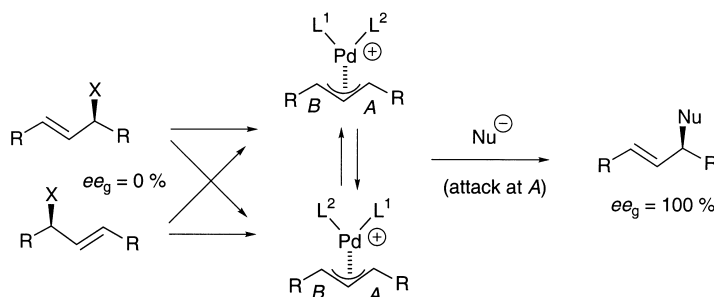
generate allylic intermediates in which there is identical 1,3-substitution, such that the π -allylpalladium intermediate contains a 'meso' allyl fragment that is desymmetrised by the chiral Pd-ligand assembly. Both enantiomers of substrate should generate the same set of equilibrating intermediates and thereby, under the influence of a perfect ligand, facilitate the generation of a single enantiomer of product from a racemic substrate (Scheme 1).

[a] Dr. G. C. Lloyd-Jones, Dr. I. J. S. Fairlamb
The Bristol Centre for Organometallic Catalysis
School of Chemistry, University of Bristol
Cantock's Close, Bristol BS8 1TS (UK)
Fax: (+44) 117/929 8611
E-mail: guy.lloyd-jones@bris.ac.uk
ijsf1@york.ac.uk

[b] Dr. I. J. S. Fairlamb
Current address: Department of Chemistry
University of York
Heslington, York, YO10 5DD (UK)

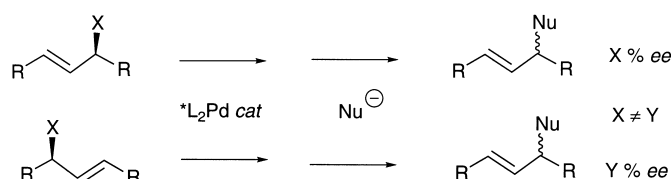
[c] Dr. Š. Vyskočil, Prof. Dr. P. Kočovský
Department of Chemistry
Joseph Black Building, University of Glasgow
Glasgow, G12 8QQ (UK)
E-mail: stepanv@natur.cuni.cz
p.kocovsky@chem.gla.ac.uk

[d] Dr. Š. Vyskočil
Department of Organic Chemistry
Charles University, 128 40
Prague 2 (Czech Republic)



Scheme 1. An allylic alkylation reaction involving a racemic, symmetrically disubstituted and thus pro-meso, electrophile in which a chiral Pd-catalyst "L¹-L²-Pd" generates a fully equilibrated set of intermediates and effects complete control over the regioselectivity of nucleophilic attack, thereby giving the substitution product in 100% *ee*.

The two most commonly employed substrates are racemic 1,3-diphenylpropenyl esters and cycloalk-2-enyl esters. Because of the importance of torquoselectivity^[2] in the product-determining step, the latter substrates, which generate slim cyclic (*anti,anti*-allyl) intermediates, provide a significantly more challenging testing ground for ligand efficacy. The use of a chiral but racemic substrate adds the complication that the catalyst may react with the two enantiomers of substrate in an enantiodiscriminatory manner (i.e. be 'matched and mismatched'). In the simplest case, one enantiomer may be converted faster than the other (i.e. kinetic resolution occurs) but due to the generation of 'meso' intermediate(s) the enantiomeric excess (*ee*) of the product is the same irrespective of its enantiogenesis. However, it was reported by Fiaud and Malleron some 20 years ago^[3] that with certain catalysts, the two enantiomers of substrates may give products of different enantiomeric excess (*X* %, *Y* %, Scheme 2).

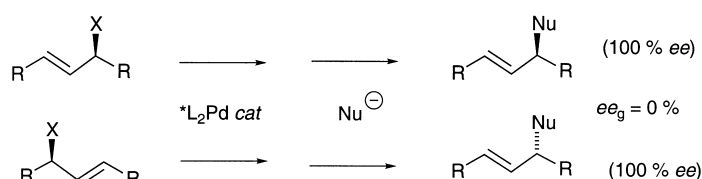


Scheme 2. The same type of reaction as in Scheme 1, but in which there is an imperfect memory effect and thus enantiomeric substrates give products of different enantiomeric excess.

This phenomenon, or more generally, the situation in which reaction of isomeric allylic substrates does not obey the classical mechanism to give identical product ratios, has become known as a 'memory effect'. More recently, the

Abstract in Czech: Je prezentován kvantitativní popis paměťového efektu při palladiem katalyzované allylové substituci, která formálně probíhá přes 'meso' π -allylové intermedie. Užitečnost tohoto popisu [stereochemická konvergence (*sc*) a globální enantiomerní přebytek (ee_g)] je ukázána při jeho aplikaci na serii palladiem katalyzovaných allylových alkylačních reakcí racemických cyklopentenylových esterů. Analýza takových reakcí s použitím řady enantiomerně čistých monofosfinových ligandů podporuje závěr, že selektivity (*ee*) získané za standardních podmínek mohou být velmi zvláštní, uplatňuje-li se zároveň silný paměťový efekt. Porovnáním *sc* a *ee* pro danou kombinaci ligandu a rozpouštědla za různých podmínek lze však předpovědět limitní (latentní) selektivitu, které by bylo dosaženo v případě potlačení paměťového efektu. Tato analýza je demonstrována na příkladu jednoho z ligandů (**4b**, 'MAP'), pro nějž byla použita řada postupů k definování podmínek, které potlačují paměťový efekt, což vede k odhalení limitní selektivity. Za těchto podmínek lze dosáhnout vyšší limitní globální selektivity, než jaká je dosažitelná při použití standardní metody ekvibrace diastereoisomerů, jakou je např. přidavek halidového iontu. Analýza *sc* proti ee_g tak rovněž umožňuje rozlišit drobné změny v selektivitě. Původ rozdílů v limitní selektivitě (za přítomnosti a při absenci chloridu) lze hledat v rozdílné reaktivitě neutrálních monodentálních a kationoidních bidentálních komplexů MAP (**4b**) a MOP (**4b**).

implication that undetected memory effects may compromise accurate ligand 'benchmarking', *vide infra*, and the possible utility of memory effects has resulted in more widespread study.^[4] Despite this attention, the origins of such memory effects are still a matter of debate and a number of potential factors, which undoubtedly vary from system to system, have been identified.^[4] These include asymmetric ion-pairing,^[5] slow diastereoisomer equilibration,^[4c, 6] monomer–oligomer equilibria,^[7] multiple bidentate coordination modes^[8] and σ -allyl versus π -allylpalladium intermediate equilibria.^[3] Irrespective of the origin of the memory effect, it is evident that *complete* ('perfect') stereochemical memory in a quantitative reaction involving a racemic substrate *must* result in a racemic product (Scheme 3).



Scheme 3. The same type of reaction as in Scheme 2, but here the memory effect is perfect, each enantiomeric substrate giving the substitution product in 100% *ee*. The net selectivity (global enantiomeric excess, ee_g) is thus 0%.

However, away from this limiting regime (e.g. Scheme 2), the description of the memory effect (the extent of the disparity between the stereochemical outcome of enantiomeric substrates) is usually limited to 'weak', 'medium' or 'powerful'. Herein we introduce an alternative and quantitative two-term description: stereochemical convergence (*sc*) and global enantiomeric excess (ee_g). We then demonstrate the utility of this two-term description by study of the enantiomeric excesses obtained under typical conditions for the Pd-catalysed allylic alkylation reaction of cyclopentenyl substrates employing a range of chiral enantiomerically pure P,X ligands. With some ligands, powerful memory effects are observed and in these cases, analysis of the change in ee_g with *sc*, when reactions conditions are varied, allows some conclusions to be drawn regarding neutral versus ionic intermediates.

Results and Discussion

Description and quantification of memory effects in asymmetric Pd-catalysed allylation: Consider the quantitative reaction of a racemic allyl substrate '(±)-S', with a nucleophile ('Nu'), proceeding via 'meso'-type allylpalladium intermediate(s), to give (–)- and (+)-enantiomers of product 'P', catalysed by an enantiomerically pure Pd species whose *intrinsic selectivity* (i.e. in the complete absence of any memory effect) favours generation of (+)-P. The results from such a reaction can be plotted on a graph where the x and y axes represent the outcome (*ee* of product P) from the reaction of one enantiomer of substrate (S) versus the other.

With reference to a plot of the *ee* of **P** from (+)-**S** (*ee* (+)-**P**₍₊₎, *x* axis) against the *ee* **P** from (–)-**S** (*ee* (+)-**P**_(–), *y* axis; Figure 1), three important regions can be identified. The first

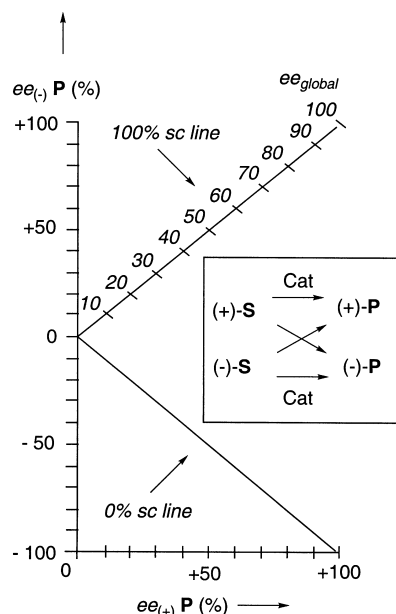


Figure 1. Plot, with reference to Scheme 1, Scheme 2 and Scheme 3, of enantiomeric outcome (*ee*) from reaction of the 'matched' enantiomer of substrate ((+)-**P**₍₊₎, *x* axis) versus that of the 'mismatched' enantiomer ((+)-**P**_(–), *y* axis). The two diagonal lines show points of complete (100%) stereochemical convergence (*sc*) and divergence (0% *sc*). See text for full discussion.

is located along the solid line between (0,0) and (+100, +100). Since the term *stereoconvergent*^[9] is applied to a reaction in which stereoisomerically differing starting materials yield identical products, one may describe this situation as one of full stereoconvergence, that is 100% *sc*. Notably, the overall outcome (*ee*_g), which has no dependence on the enantiomeric identity or the *ee* of substrate **S**, is determined solely by the efficacy of the ligand–palladium assembly and represents the intrinsic selectivity of the system. The *ee*_g varies linearly along the 100% *sc* line between (0,0; *ee*_g = 0%) and (100, 100; *ee*_g = 100%). This situation is usually presumed to prevail when these reactions are employed for 'benchmarking' of ligands. The second region lies at the other extreme and is represented by the solid line between coordinates (0,0) and (+100, –100). Points on this line represent a stereospecific^[9] reaction in which there has been no stereoconvergence and the line may thus be labelled 0% *sc*. In other words, the extent with which the stereochemical pathways of reaction of (+)-**S** and (–)-**S** have converged is 0% and the two reaction manifolds mirror each other exactly. Notably, only when the outcome is (+100, –100) is there a *perfect* stereochemical memory effect in as much as (+)-**S** gives, for example, (+)-**P**₍₊₎ (100% *ee*) whilst (–)-**S** gives (–)-**P**_(–) (100% *ee*). However, in all cases on the 0% *sc* line the global *ee* is zero (*ee*_g = 0), provided that there has been equimolar conversion of (–)-**S** and (+)-**S**. If this is not the case, for example in reactions involving non-racemic substrate, or kinetic resolution, then there will be a non-zero global *ee*.

The third and final region is the outcome between these two extremes and is more complex: there is a memory effect; however, it is not equal between matched^[10] and mismatched manifolds and thus there is partial asymmetric induction, that is *ee*_g **P** ≠ 0. We suggest that such situations may be described in a useful and quantitative manner by reporting the degree of stereochemical convergence (*sc* [%]) and the resulting global enantiomeric excess (*ee*_g [%]); *sc* and *ee*_g are calculated mathematically and then compared, between reactions, graphically. The value of *sc* is simply calculated from the stereochemical outcome from one enantiomer of substrate against a sliding scale which varies in response to the outcome from the other enantiomer. Thus for the hypothetical example above, in which (+)-**S** is matched, *sc* (%) = 100 {[(+)-**P**₍₊₎] – [(–)-**P**_(–)]} / {[(+)-**P**₍₊₎] + [(–)-**P**₍₊₎]}. As examples of the application of *ee*_g and *sc* to reaction outcomes, consider points **A** and **B**, derived from hypothetical data from a reaction of (±)-**S** to give **P**, performed with the same chiral ligand, same nucleophile and solvent, but under different conditions, for example using different Pd catalyst precursors (Figure 2). Note that in this figure, lines of equal *sc*

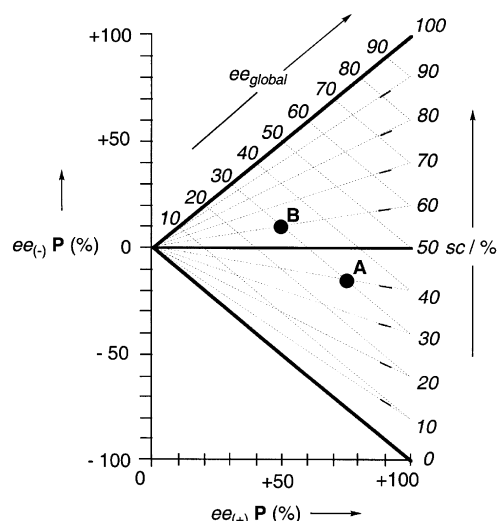


Figure 2. Framework from Figure 1, with addition of 1) dashed-line 'contours' of stereochemical convergence (see text) and global *ee* and 2) hypothetical data sets (**A**, **B**) from a reaction displaying a memory effect. See text for full discussion.

(from 10 to 90%) have been highlighted by dashes that radiate out from the origin (0,0), whilst lines of equal *ee*_g have been highlighted by dashes that lie parallel to the 0% *sc* line (0,0 to 100, –100). Under conditions **A**, matched enantiomer (+)-**S** gives (+)-**P**₍₊₎ in 75% *ee* (*x* axis) and (–)-**S** gives the *opposite* enantiomer, (–)-**P**_(–), in 15% *ee* (*y* axis). Thus the global *ee*_g is 30% (in favour of (+)-**P**) and the stereochemical convergence *sc* is 40%. Changing to conditions **B** affects the outcome from both enantiomers: matched (+)-**S** gives (+)-**P**₍₊₎ in 50% *ee* and mismatched (–)-**S** now gives the same enantiomer, (+)-**P**_(–), in 10% *ee*. The global *ee* is still 30%, but the stereochemical convergence has increased to 60% *sc*. The relationship between these two results (**A** and **B**) is more easily visualised as *sc* (*x* axis) versus global *ee*_g (*y* axis) (Figure 3).

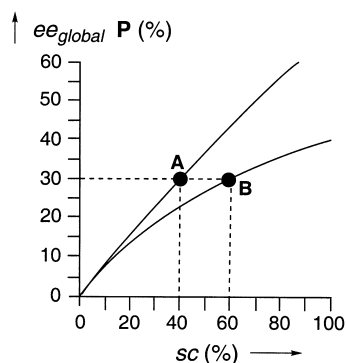
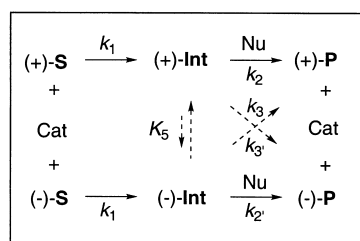
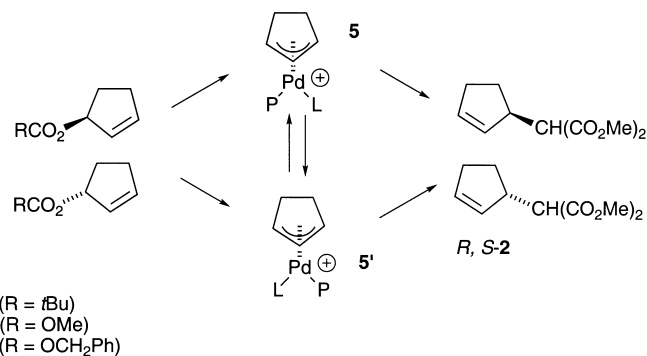


Figure 3. A re-plot of the hypothetical data sets (**A**, **B**), from Figure 2, on axes of stereochemical convergence (*sc*, *x* axis) versus global *ee_g* (*y* axis). The curves passing through the points are predicted *sc* versus *ee_g* relationships for a hypothetical reaction (see inset) in which there is the possibility of memory effects. See experimental section for full details of kinetic models. For the curve passing through **A**, (+)-**Int** is favoured over (–)-**Int** ($K^{-1}=6$), (+)-**Int** reacts with 80% diastereoselectivity and (–)-**Int** with 66% diastereoselectivity for the curve passing through **B**, (+)-**Int** is favoured over (–)-**Int** ($K^{-1}=3$) and both react with 80% diastereoselectivity. Memory effects (*sc*) are modulated by variation in k_5/k_{-5} .

Simulation of the kinetics for a reaction (see inset to Figure 3) in which the memory effect is attenuated (i.e. *sc* increased) through increasing the extent of first-order equilibration of diastereoisomeric intermediates “(+)-**Int** and (–)-**Int**” before nucleophilic attack, indicates that a simple relationship will exist between *sc* and *ee_g*. The relationship takes the form of a curve, whose origin is *sc*=*ee_g*=0 when diastereoselectivity of attack of (+)-**Int** and (–)-**Int** is equal and opposite. Considering points **A** and **B**, it is evident that they *must* lie on different curves since they produce identical *ee_g* but have different *sc*. The generation of differing *sc* versus *ee_g* relationships is only feasible when the *intrinsic* selectivity of the catalyst system is different. In this case the catalyst system operative under conditions **A** displays higher net intrinsic selectivity than that operative under **B**. In other words, having taken into account the memory effect (by *sc*), comparison of the data for **A** and **B** demonstrates that the two reactions must proceed via different intermediates. It should be noted that in the absence of analysis of the memory effect (i.e. stereochemical convergence), the data available from ‘experiments’ **A** and **B** would solely be that product (+)-**P** of the same *ee* (30% *ee*) is obtained.

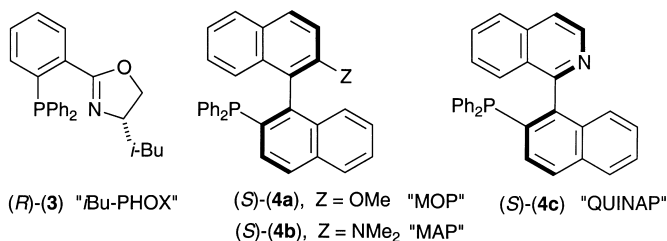
Herein we demonstrate the utility of stereochemical convergence analysis by study of the relationship between *sc* and *ee* for the reaction **1** → **2** (Scheme 4).^[11]

Assessing ligands 3, 4a, 4b and 4c under “benchmarking” conditions: Under standard conditions for ‘benchmarking’ (THF, 25 °C, 5 mol % ligand, 2.5 mol % [PdCl(π-C₃H₅)₂],



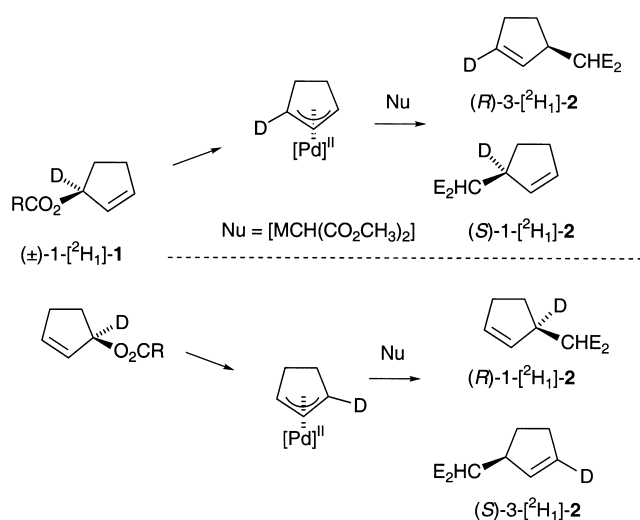
Scheme 4. Pd-catalysed allylic substitution of cyclopentenyl esters **1a**, **1b** and **1c** with a malonate type nucleophile, catalysed by a Pd-complex bearing a mono-phosphine ligand (L = N, C, halide), to give **2** via diastereoisomeric intermediates **5** and **5'**.

‘Pd(L)’ complexes of the enantiomerically pure ligands (*R*)-**3**, (*i*Bu-**PHOX**),^[12] (*S*)-**4a** (‘**MOP**’),^[13] (*S*)-**4b** (‘**MAP**’)^[4c,14] and (*S*)-**4c** (‘**QUINAP**’)^[15] catalyse the reaction of racemic cyclopentenyl pivalate (±)-**1a** with sodium dimethyl malonate [NaCH(CO₂Me)₂; 2 equivalents] to give allylic alkylation product (*R*)-**2** in 8, 22, 10 and 36% *ee_g*, respectively. These



results suggest that of the four ligands, ‘**QUINAP**’ ((*S*)-**4c** → 36% *ee*) is the best candidate for optimisation with ‘**MOP**’ ((*S*)-**4a** → 22% *ee*) a poor second choice and ‘*i*Bu **PHOX**’ ((*R*)-**3** → 8% *ee*) or ‘**MAP**’ ((*S*)-**4b** → 10% *ee*) of little potential utility in this reaction.

However, the above benchmarking reactions have been analysed without taking into consideration the possibility of memory effects. To test for memory effects one must individually assess the outcome from both enantiomers of substrate (**1a**). This cannot be achieved with racemic **1a** since either enantiomer of **2** can arise from either enantiomer of **1a**, indeed this is the very principle on which this type of asymmetric process is based. However, employing enantiomerically pure **1a** is not ideal since a) two reactions must be performed to assess the outcome from both enantiomers, b) both enantiomers of **1a** (or of the ligand) must be readily available in very high *ee* and c) due to match/mismatch effects, the reaction outcomes involving pure enantiomers may differ from that of the racemate. To address the above issues, we have developed the use of isotopic desymmetrisation.^[4b,16] This facilitates *simultaneous* analysis of the individual contributions to the global *ee_g* from (*R*)-**1a** and (*S*)-**1a** through deployment of a racemic, deuterium labelled^[17] substrate (±)-1-[²H]₁-**1a** (Scheme 5).



Scheme 5. The “isotopic desymmetrisation” technique employed to simultaneously compare stereochemical outcomes in the Pd-catalysed allylic substitution of cyclopentenyl esters (**1**). The racemic deuterium labelled substrate (\pm)-1-[$^2\text{H}_1$]-**1** undergoes *stereospecific* substitution (net retention) and thus (*R*)-1-[$^2\text{H}_1$]-**1** gives only (*R*)-1-[$^2\text{H}_1$]-**2**/(*S*)-3-[$^2\text{H}_1$]-**2** and analogously (*S*)-1-[$^2\text{H}_1$]-**1** gives only (*S*)-1-[$^2\text{H}_1$]-**2**/(*R*)-3-[$^2\text{H}_1$]-**2**. The relative population of the four isotopomeric enantiomers of 1,3-[$^2\text{H}_1$]-**2** can be assayed by $^{13}\text{C}\{^1\text{H}\}$ NMR in the presence of (+)-[Eu(hfc) $_3$].

When this technique is applied to the reactions discussed above, it sheds a rather different light on the situation (Table 1, entries 1, 3, 5 and 7). With the (*P,N*)-ligands *i*Bu PHOX (**3**) and QUINAP (**4c**) there are memory effects (67 and 82 % *sc*) but these are weak and the global *ee_g* values (8 % and 36 % *ee*, respectively) closely reflect the intrinsic or limiting selectivity of the ligand systems under these conditions (Table 1, entries 1 and 3). When the same reactions are conducted in the absence of chloride, catalytic activity is reduced substantially (Table 1, entries 2 and 4). In stark contrast, with the ligands MOP (**4a**) and MAP (**4b**) much more powerful memory effects are apparent under ‘benchmarking’ conditions: 28 % *sc*, 22 % *ee_g*, with MOP (**4a**) and 15 % *sc*, 10 % *ee_g*, with MAP (**4b**) (Table 1, entries 5 and 7). Furthermore, in the absence of halide, catalytic activity remains high and the memory effects are very slightly increased (Table 1, entries 6 and 8).

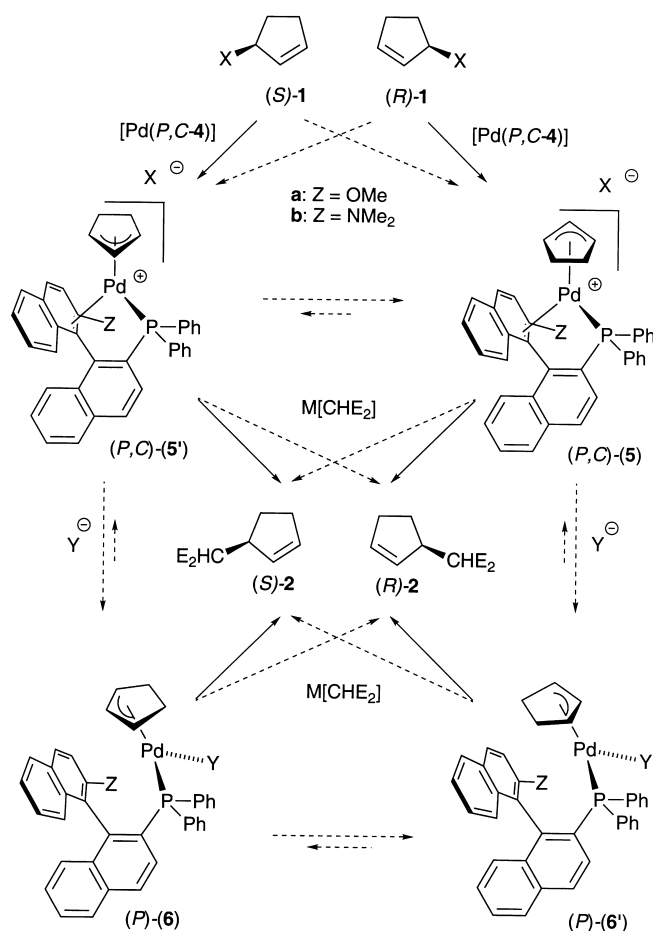
It is a common misconception that the ligands MOP (**4a**) and MAP (**4b**) are exclusively monodentate phosphine ligands. In fact, when either ligand coordinates a Pd^{II} centre that has two free coordination sites (i.e. it bears only two other ligands, e.g., two chlorides or a $\pi\text{-C}_3\text{H}_5$ unit) a bidentate (*P,C*)-coordination mode is established by coordination of Pd to the

Table 1. Allylic alkylation of cyclopentenyl esters (\pm)-1-[$^2\text{H}_1$]-**1a–c** (0.125 M) in THF, 25 °C, with [NaCH(CO $_2$ CH $_3$) $_2$] (preformed, added slowly, or generated in situ) catalysed by 5 mol % Pd/ligand (*i*Bu PHOX (**3**), MOP (**4a**), MAP (**4b**) or QUINAP (**4c**), to give 1,3-[$^2\text{H}_1$]-**2** (see Scheme 5).

Entry ^[a]	R	Ligand	Cl ^[b] [mol %]	Nu. ^[c]	Additive ^[d] [mol %]	Time ^[e] [h]	<i>sc</i> [%] ^[f]	1,3-[$^2\text{H}_1$]- 2 <i>ee_g</i> [%] ^[g]	yield [%] ^[h]
1	Me ^[i]	(<i>S</i>)- 3	5	pref.	– ^[j]	< 0.08	67	8 (<i>R</i>)	88
2	<i>t</i> Bu	(<i>S</i>)- 3	–	pref.	– ^[j]	48	> 95	6 (<i>R</i>)	8 ^[k]
3	<i>t</i> Bu	(<i>S</i>)- 4c	5	pref.	– ^[j]	2.25	82	36 (<i>R</i>)	82
4	<i>t</i> Bu	(<i>S</i>)- 4c	–	pref.	– ^[j]	12	–	–	0 ^[l]
5 (IIi)	<i>t</i> Bu	(<i>S</i>)- 4a	5	pref.	– ^[j]	< 0.08	28	22 (<i>R</i>)	82
6 (Ii)	<i>t</i> Bu	(<i>S</i>)- 4a	–	pref.	– ^[j]	< 0.08	26	20 (<i>R</i>)	86
7 (IIi)	<i>t</i> Bu	(<i>S</i>)- 4b	5	pref.	– ^[j]	< 0.08	15	10 (<i>R</i>)	85
8 (Ii)	<i>t</i> Bu	(<i>S</i>)- 4b	–	pref.	– ^[j]	< 0.08	10	8 (<i>R</i>)	80
9 (Iii)	<i>t</i> Bu	(<i>S</i>)- 4b	–	pref.	F (5)	< 0.08	16	14 (<i>R</i>)	85
10 (IIii)	<i>t</i> Bu	(<i>S</i>)- 4b	–	slow.	– ^[j]	0.25	35	23 (<i>R</i>)	56
11 (Iiv)	<i>t</i> Bu	(<i>S</i>)- 4b	–	slow.	– ^[j]	0.5	70	44 (<i>R</i>)	44 ^[m]
12 (Iv)	OMe	(<i>S</i>)- 4b	–	pref.	– ^[j]	< 0.08	89	52 (<i>R</i>)	42
13 (Ivi)	OBn	(<i>S</i>)- 4b	–	pref.	– ^[j]	< 0.08	99	58 (<i>R</i>)	39
14 (Ivii)	OMe	(<i>S</i>)- 4b	–	in situ	NaOMe (1)	< 0.17	95	55 (<i>R</i>)	89
15 (Iviii)	OBn	(<i>S</i>)- 4b	–	in situ	NaOAc (1)	1	98	57 (<i>R</i>)	80
16 (IIii)	<i>t</i> Bu	(<i>S</i>)- 4a	–	slow	– ^[j]	0.5	60	35 (<i>R</i>)	32
17 (Iiv)	OMe	(<i>S</i>)- 4a	–	pref.	– ^[j]	< 0.08	91	52 (<i>R</i>)	34
18 (Iv)	OMe	(<i>S</i>)- 4a	–	in situ	NaOAc (1)	1	92	56 (<i>R</i>)	73
19 (IIii)	<i>t</i> Bu	(<i>S</i>)- 4b	5	slow	– ^[j]	0.5	42	22 (<i>R</i>)	69
20 (IIiii)	OBn	(<i>S</i>)- 4b	5	pref.	– ^[j]	16	58	30 (<i>R</i>)	20 ^[n]
21 (IIiv)	OMe	(<i>S</i>)- 4b	5	in situ	NaOMe (1)	36	84	26 (<i>R</i>)	22 ^[o]
22 (IIv)	OBn	(<i>S</i>)- 4b	5	in situ	NaOMe (1)	1	98	44 (<i>R</i>)	30 ^[p]
23 (IIv)	OBn	(<i>S</i>)- 4b	5	in situ	NaOAc (1)	48	–	–	0 ^[l]

[a] Lower case italics (*i*, *ii*, *iii* etc.) refer to individual points in graphs (**I** and **II**) of *sc* versus *ee_g*; see Figure 4. [b] 5 mol % Cl is present from generation of the pro-catalyst in situ by reaction of ligand (5 mol %) with [Pd $_2$ ($\eta^3\text{-C}_3\text{H}_5$) $_2\text{Cl}_2$]; – refers to use of [($\pi\text{-C}_3\text{H}_5$)Pd(L)][O $_3\text{SCF}_3$] as pro-catalyst. [c] Nucleophile is preformed [NaCH(CO $_2$ Me) $_2$] (2.0 equiv) and added in one portion (“pref.”), added slowly by syringe pump (“slow”) or generated in situ from MX (additive) and CH $_2$ (CO $_2$ Me) $_2$ (2.0 equiv; “in situ”). [d] Additive present to effect equilibration (F $^-$) or generate nucleophile (NaOMe) or activate pro-catalyst (NaOAc or LiOAc). [e] Time at which TLC analysis showed complete consumption of substrate (unless otherwise noted). [f] Determined by ^{13}C NMR analysis; *sc* (%) = 100 [(*R_R* – *S_S*)/(*R_R* + *S_S*)] where mol fractions of enantiomeric products *R_R*-(**2**) and *S_R*-(**2**) are obtained from *R*-(**1**) (and *R_S*-(**2**) and *S_S*-(**2**) from (*S*)-**1**). [g] Determined by ^{13}C NMR analysis; *ee_g* = global *ee* of overall sample of 1,3-[$^2\text{H}_1$]-**2**. [h] Yield of analytically pure 1,3-[$^2\text{H}_1$]-**2** obtained after chromatography on silica gel. In some cases, as noted, starting material (1-[$^2\text{H}_1$]-**1**) was recovered as a single regioisotopomer. [i] Acetate instead of pivalate was employed. [j] No additive. [k] Low extent of conversion; substrate recovered in 47 % yield. [l] No product detected by TLC; substrate recovered in quantitative yield. [m] Substrate recovered in 40 % yield. [n] Substrate recovered in 41 % yield. [o] Substrate recovered in 25 % yield. [p] Substrate recovered in 36 % yield.

C(1)=C(2) bond of the *non*-phosphine bearing aryl ring. This (*P,C*) coordination mode is observed in both the solid state (X-ray analysis) and in solution (NMR spectroscopy), for example in the complexes $[(\pi\text{-C}_3\text{H}_5)\text{Pd}(\text{P},\text{C-4a})][\text{O}_3\text{SCF}_3]$ and $[(\pi\text{-C}_3\text{H}_5)\text{Pd}(\text{P},\text{C-4b})][\text{O}_3\text{SCF}_3]$.^[4c, 14b] In the former complex, the bonding to C(1)=C(2) is more η^2 - in character and in the latter complex it is essentially η^1 (tetrahedral at C(1)–Pd). We have employed these complexes as analogues of non-isolable **5** ($[(\pi\text{-C}_5\text{H}_7)\text{Pd}(\text{P},\text{C-4ab})][\text{X}]$), which are postulated intermediate in the reaction of **1** \rightarrow **2**, catalysed by “Pd(**4ab**)” (Scheme 6). Study of the structure and stereodynamics of $[(\pi$



Scheme 6. The working model for powerful memory effects, and their attenuation (see text for full discussion) for the reaction shown in Scheme 4. Key to the working model is the generation of two primary cationic bidentate *P,C*-intermediates (**5** and **5'**) in a diastereoselective manner (from **(R)-1** and **(S)-1** respectively), which interconvert slowly but are attacked rapidly by malonate nucleophile at the position *trans* to P. The intermediates may also undergo ion-pair collapse to give neutral monodentate *P* complexes **6** and **6'**, which display analogous slow interconversion and selective nucleophilic attack.

$(\pi\text{-C}_3\text{H}_5)\text{Pd}(\text{P},\text{C-4ab})][\text{O}_3\text{SCF}_3]$ suggested that the powerful memory effects, and thus low *sc*, in the reaction of **1a** \rightarrow **2**, catalysed by “Pd(**4ab**)” arises by three linked events: a) enantiodivergent ionisation of **1a** by $[\text{Pd}(\text{P},\text{C-4ab})]$ such that P is located *trans* to the nucleofuge (the ‘ α -site’) leading to opposite diastereoisomers (**5b** and **5b'**) from **(R)-1a** and **(S)-1a** (Scheme 6); b) slow interconversion of the resulting ion-paired^[18] intermediates (predominantly via bidentate

(*P,C*)/monodentate (*P*-) equilibrium facilitating P–Pd rotation in the monocoordinated state) and c) rapid nucleophilic capture (again *trans* to P at the ‘ α -site’) of highly electrophilic cations **5b** with **5b'** before full equilibration has occurred.^[4c]

Hayashi and co-workers have also investigated the powerful memory effects observed in Pd-catalysed allylic alkylations involving cycloalkenyl type electrophiles when employing ligand **4a** (MOP).^[6b] The origin of the memory effect was analogously ascribed to ionisation *trans* to P, followed by slow diastereoisomer interconversion unable to compete with rapid capture (*trans* to P) by the nucleophile. However, based on Pd complexes observed (NMR) on mixing **4a** with allylpalladium chloride species, neutral and monodentate complexes (**6a** and **6a'**, Y = Cl) were postulated as intermediates. Since these powerful memory effects (as low as 10% *sc*) can also be obtained under chloride-free conditions, *vide supra*, we have postulated that under these conditions the primary ionisation products are the ion-paired intermediates **5/5'** where the counterion X is the nucleofuge. Subsequently, in competition with nucleophilic attack, these may, or may not, collapse (potentially reversibly) to neutral species **6/6'** where the counterion “Y” might be the nucleofuge (X) or a prior spectator ion. Furthermore, if the pro-catalyst bears a chloride, then catalysis may proceed via oxidative addition of **1** to a palladate type species, “[Pd(Cl)(**4ab**)][–]”, in which case the primary intermediate would be **6/6'**, i.e. generated directly rather than via **5/5'**. Whether the nucleophile attacks the cationic species **5** or the neutral mono-coordinated **6** is an important issue: in the former complex the chelated ligand will exert greater control over the regioselectivity of the nucleophilic attack, and thus the *ee* of product **2**. Thus far, it has been difficult to draw conclusions due to the powerful memory effects which mask the intrinsic selectivities and induce low *ee* (compare Table 1 entries 5 and 6 or entries 7 and 8). Here, analysis of *sc* may be of aid. Thus, if conditions are found where the system is allowed to begin to equilibrate before attack of the nucleophile, then a simple relationship between *sc* and *ee* should be observed if reaction occurs exclusively through **5/5'**: greater mixing (higher *sc*) facilitating higher *ee* until the limiting *ee* is reached at 100% *sc*. Alternatively, if collapse to **6** is in competition with equilibration and nucleophilic attack, then slowing nucleophilic attack will lead to greater reaction via **6** and thus a different relationship between *sc* and *ee*.

Attenuation of the memory effect: analysis of stereochemical convergence (*sc*) with ‘MAP’ and ‘MOP’ ligands: The outcome from a number of reactions of **1** involving catalysis by Pd(**4a**) and Pd(**4b**) under a number of (halide-free) conditions, see below, have been plotted as *sc* versus *ee*_g in Figure 4, graph I. The starting points *i* are taken from entries 6 and 8 in Table 1, in which reaction is conducted by adding the pro-catalyst $[(\pi\text{-C}_3\text{H}_5)\text{Pd}(\text{P},\text{C-4ab})][\text{O}_3\text{SCF}_3]$ to a solution of **1a** and 2.0 equivalents of $[\text{NaCH}(\text{CO}_2\text{CH}_3)_2]$ in THF.

Employing a working model for catalytic turnover which involves initial formation of an approximately 50/50 ratio of diastereoisomeric **5/5'** (i.e. $[(\pi\text{-C}_5\text{H}_7)\text{Pd}(\text{P},\text{C-4b})][\text{X}]$) from **(R)-1**/**(S)-1**, see Scheme 6, one may consider at least four variables that will affect the *sc* and thus memory effect: a) the

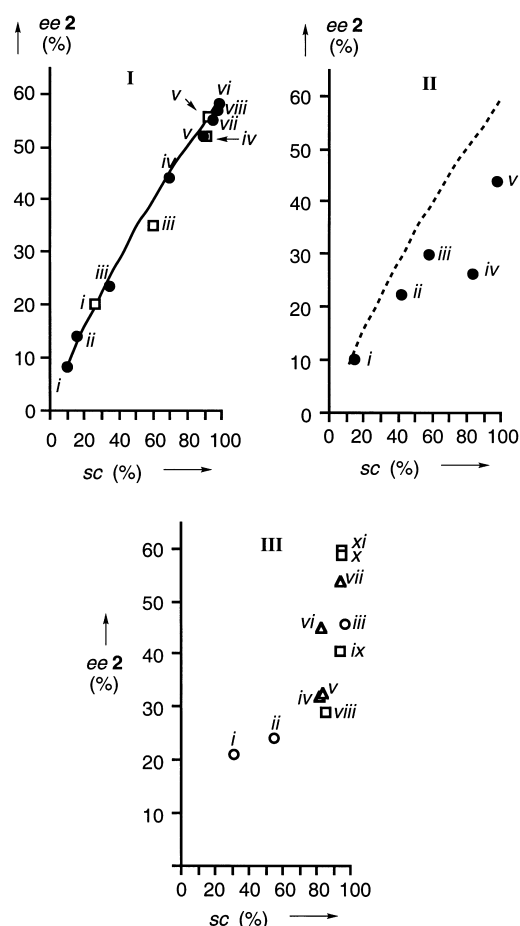


Figure 4. Variation of global enantioselectivity (ee_g-2) with stereochemical convergence ($sc-2$), as measured by isotopic desymmetrisation (see Scheme 5), for the reaction of $(\pm)-1-[^2H_3]-1a-c$ (0.125 M in THF) with “[MCH(CO₂CH₃)₂]” at 20 °C, catalysed by 5 mol % ‘Pd-4b’ or ‘Pd-4a’ under a variety of conditions (see text and Table 1 (graphs I and II) and Table 2 (graph III) for full details). In graphs I and II, closed circles relate to use of ‘Pd-4b’ and open squares to ‘Pd-4a’. In graph III, all runs employ ‘Pd-4b’ and open triangles relate to M = “EtZn”; open circles to M = “Cs” and open squares to M = “Li”. The solid curved line in graph I is the sc versus ee_g relationship predicted for **2**, employing the model outlined in the inset to Figure 3 and in which (+)-**Int** is favoured over (–)-**Int** ($K^{-1} = 7$). (+)-**Int** reacts with 88 % diastereoselectivity and (–)-**Int** with 80 % diastereoselectivity. The line is reproduced (dashed line) in graph II for comparison with the data obtained in the presence of 5 mol % chloride ion.

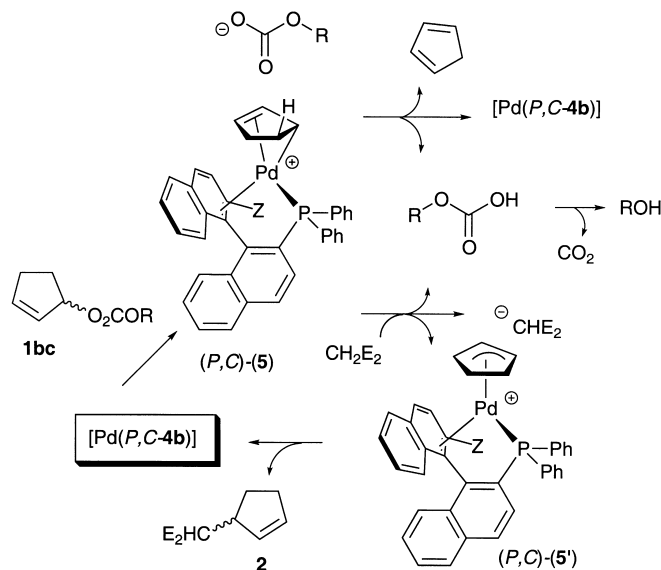
presence of reversibly coordinating additives, such as halides or dibenzylideneacetone (dba) may accelerate diastereoisomer equilibration^[6a] (i.e. **5** with **5'**) and increase sc ; b) if diastereoisomer equilibration is (pseudo)unimolecular^[19] whilst nucleophilic attack bimolecular, then lower concentrations of nucleophile [MCH(CO₂CH₃)₂] should increase sc ; c) the identity of X (the counter-ion) will affect the tightness of ion pairing in **5/5'**. This may modulate the rate of diastereoisomer equilibration and also the reactivity towards the nucleophile. It may also induce ion-pair collapse to **6/6'**; d) the identity of M (the ‘escort’ cation) will affect the reactivity of the nucleophile and lower reactivities should lead to higher sc . Furthermore, changing M may change the intrinsic selectivity of the system—as has been proposed for other systems.^[20]

We have earlier^[4c] explored variable a) above with **1a** as substrate, in general finding the effect rather small. For example, in the presence of 5 mol % fluoride^[21] (Table 1, entry 9) the sc increases slightly from 10 % to 16 % (see point ‘ii’ in graph I; Figure 4). It is clear that **5/5'** (X = O₂CtBu) displays a high reactivity towards [NaCH(CO₂CH₃)₂] and thus we now consider variable b): the effect of the concentration of nucleophile (Table 1, entries 10 and 11). Again employing $[(\pi-C_3H_5)_2Pd(P,C-4b)][O_3SCF_3]$ as pro-catalyst, slow addition (via syringe pump) of one equivalent of [NaCH(CO₂CH₃)₂] in THF caused the sc to rise (15 min. addition: 35 % sc ; 30 min. addition: 70 % sc (see points ‘iii’ and ‘iv’, graph I; Figure 4). However, after complete addition there was still substrate^[22] present and thus yields of **2** were low (56 and 44 % respectively) and when slow addition of [NaCH(CO₂CH₃)₂] was performed over 1 h, no conversion of **1a** to **2** occurred at all.

Turning then to variable c), we switched from a pivalate nucleofuge to methyl carbonate (i.e. **1b**) so that intermediates of type $[(\pi-C_3H_5)_2Pd(P,C-4b)][X]$, where X = MeOCO₂[–] or MeO[–] would be generated. The latter alkoxide would arise through decarboxylation and would form a significantly tighter ion-pair than carboxylate with the cationic complex. Such tight ion-pairing would undoubtedly affect both the reactivity and rate of diastereoisomeric equilibration of the intermediates. The effect of changing from ester to carbonate^[23] was dramatic since complete consumption of **1b** and even higher stereochemical convergence could be attained (89 % sc) without the need for slow addition (Table 1, entry 12; point ‘v’, graph I; Figure 4). Interestingly, if this reaction had been performed under standard benchmarking conditions (i.e. without studying the memory effect) then, because the global selectivity is now $ee_g = 52$ % (rather than $ee_g = 10$ % ee with **1a**), one might have concluded that the change in leaving group had affected the *intrinsic* selectivity of the system. In fact, this is not the case since the simple relationship between sc and ee_g has been maintained and the increased ee arises through increased interconversion of diastereoisomeric intermediates before nucleophilic attack.

Although the sc increased on changing to **1b**, the yield was only 42 %—despite complete consumption of substrate. This is substantially lower than with **1a** where yields were in the range 80–85 %. A slightly bulkier carbonate (benzyl carbonate **1c**) was also prepared. This proved to be slightly better than **1b** (Table 1, entry 13): again, slow addition of [NaCH(CO₂CH₃)₂] was not required to achieve very high sc (99 %) with 58 % ee_g (point ‘vi’, graph I; Figure 4) but again reaction proceeded in poor yield (39 % yield of **2**, > 99 % conversion of **1c**). By study of the reaction mixtures *in situ* (¹H NMR, 500 MHz) we traced the low yields with **1b** and **1c** to a competing elimination reaction caused by the carbonate or alkoxide co-products (RCO₂Na or RONA; R = Me or Bn). This side reaction was exacerbated by low nucleophile concentration. For example, when [NaCH(CO₂CH₃)₂] was added as a solid to a solution of **1b** and $[(\pi-C_3H_5)_2Pd(P,C-4b)][O_3SCF_3]$ (5 mol %) in [D₈]THF, > 90 % conversion of **1b** to cyclopentadiene (identified by reference to a sample of freshly ‘cracked’ dimer) occurred in less than 1 min, at which point very little [NaCH(CO₂CH₃)₂] had dissolved. General

base-mediated β -elimination in allylpalladium complexes has been documented^[24] and the Pd-catalysed conversion of **1b** (or **1c**) to cyclopentadiene likely proceeds through an analogous process as outlined in the upper section of Scheme 7.^[25]



Scheme 7. The generation of an ionic acid-base pair (*P,C*-5) from a carbonate substrate (**1b** or **1c**) and a [*P,C*-4b-Pd]^{II} complex. An acid–base elimination reaction results in generation of cyclopentadiene from the cyclopentenyl allyl unit, whilst interception with a malonic acid ester results in generation of a malonate anion and subsequent nucleophilic attack on the allyl.

To combat this competing β -elimination we changed from using the pre-formed nucleophile [NaCH(CO₂CH₃)₂] to using the pro-nucleophile CH₂(CO₂CH₃)₂ as an acid which could then compete with **5** for the basic nucleofuge (ROCO₂[−] or RO[−]) as shown in the lower section of Scheme 7. Because we were using a Pd^{II} complex ([(π -C₃H₅)Pd(*P,C*-4b)][O₃SCF₃]) as pro-catalyst, an initiator was required to generate the catalytic intermediate “[Pd⁰(*P,C*-4b)]”. We found that 1 mol % NaOAc worked rather efficiently through acetoxylation of the allylpalladium cation (vide infra) and, equally well, 1 mol % NaOMe, through generation of trace [NaCH(CO₂CH₃)₂] which can then alkylate the pro-catalyst. Under these conditions high *sc* could be attained (points *vii* and *viii*, graph I; Figure 4) with both **1a** and **1b**, but now with much improved yields (Table 1, entries 14 and 15). Essentially identical results were obtained with MOP (**4a**,

Table 1, entries 16–18) which gave a similar intrinsic selectivity (*ee*_g limit \approx 58 %, see open squares in graph I, Figure 4).

The effect of chloride ion: bidentate cationic (*P,C*)- versus monodentate neutral (*P*)-coordination: Chloride-bearing Pd-catalyst precursors are commonly employed in Pd-catalysed allylic alkylations and the presence of halide ion^[26] is often perceived as being of benefit to asymmetric induction since it can accelerate diastereoisomer interconversion.^[27] As a starting point, consider the original results attained under ‘benchmarking’ conditions with MAP (**4b**) (Table 1, entry 7, Figure 4, graph II, point ‘i’). Employing identical strategies to those outlined above (b and c), we were able to increase the *sc* under ‘chloride conditions’ (5 mol % Cl engendered by use of [(π -C₃H₅)Pd(Cl)(*P*)-4b]) as pro-catalyst). However, it became clear that under conditions that gave higher *sc*, chloride had quite negative effects (see graph II in Figure 4 and Table 1, entries 19–23).

With pivalate **1a**, slow addition of [NaCH(CO₂Me)₂] gave 69 % yield of **2** with 42 % *sc*, and 22 % *ee* (Table 1, entry 19, ‘ii’, graph II; Figure 4). More dramatic was the effect with the carbonate substrates under stoichiometric (entry 20, graph II, ‘iii’; Figure 4) or catalytic (entries 21 and 22, ‘iv’ and ‘v’, graph II; Figure 4) nucleophile conditions which gave low yields of **2** (20–30 %), high *sc* (58–98 %) and much lower *ee*_g (26–44 %). In the latter reactions NaOMe was employed since NaOAc was ineffective as an initiator (entry 23) for generation of “[Pd⁰(*P,C*-4b)]” from [(π -C₃H₅)Pd(Cl)(*P*)-4b].

We also briefly studied the effect of (formal) nucleophile escort cation, that is variable d) above (Table 2, Figure 4, graph III). The use of stoichiometric nucleophiles [MCH(CO₂-CH₃)₂], (M = XZn, Cs, Li; Table 2, entries 2, 5–8 and 10) with **1a–c** gave variable results. Catalytic generation of nucleophile only functioned with Li (Table 2, entries 11–13) since

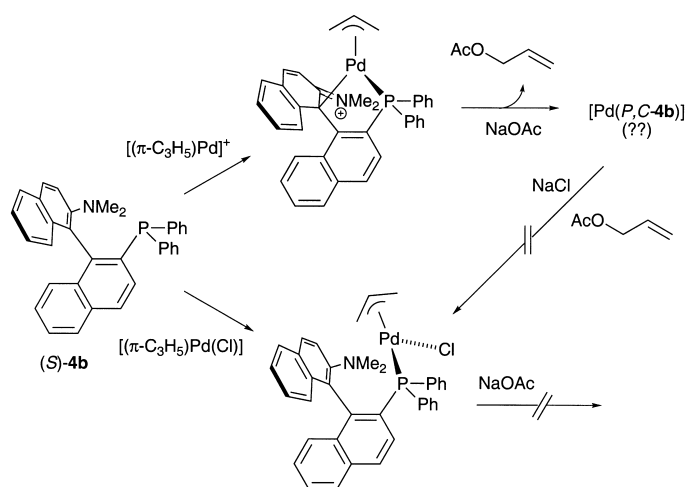
Table 2. Allylic alkylation of cyclopentenyl esters (\pm)-1-[²H]₁-**1a–c** (0.125 M) in THF, 25 °C, with [MCH(CO₂CH₃)₂] (preformed 2.0 equiv or generated in situ from CH₂(CO₂CH₃)₂) catalysed by 5 mol % Pd/ MAP (**S-4b**), to give 1,3-[²H]₁-**2** (see Scheme 5).

Entry ^[a]	R	Cl ^[b]	Nucleophile generation ^[c]	Time ^[d] [h]	<i>sc</i> [%] ^[e]	1,3-[² H] ₁ - 2 <i>ee</i> _g [%] ^[f]	yield [%] ^[g]
1 (IIIi)	<i>t</i> Bu	–	CsOAc (1 mol %)/BSA	24	31	21	36
2 (IIIii)	OMe	–	Cs ₂ CO ₃	24	55	24	23
3 (IIIiii)	OMe	–	CsOAc (1 mol %)/BSA	3	97	46	61
4	OMe	5 or 0	CsOAc (1 mol %)	24	–	–	0
5 (IIIiv)	OMe	–	Et ₂ Zn	2	82	32	78
6 (IIIv)	OMe	5	Et ₂ Zn	2	84	32	69
7 (IIIvi)	<i>t</i> Bu	–	Et ₂ Zn	3	83	45	78
8 (IIIvii)	<i>t</i> Bu	5	Et ₂ Zn	18	94	54	67
9	OMe	5 or 0	Zn(OAc) ₂ (1 mol %)	24	–	–	0
10 (IIIviii)	<i>t</i> Bu	–	BuLi	3	85	29	21
11 (IIIix)	OBn	5	LiOMe (1 mol %)	24	95	40	24
12 (IIIx)	OBn	–	LiOMe (1 mol %)	2	95	59	77
13 (IIIxi)	OMe	–	LiOMe (1 mol %)	0.17	95	60	69

[a] Lower case italics (*i*, *ii*, *iii* etc.) refer to individual points in graph III of *sc* versus *ee*_g; see Figure 4. [b] 5 mol % Cl is present from generation of the pro-catalyst in situ by reaction of **4b** (5 mol %) with [Pd₂(η ³-C₃H₅)₂Cl₂]; – refers to use of [(π -C₃H₅)Pd(**4b**)] [O₃SCF₃] as pro-catalyst. [c] Nucleophile is preformed by reaction of base (2.0 equiv) with CH₂(CO₂Me)₂ (2.0 equiv and added in one portion or generated in situ from MX (1 mol %) and CH₂(CO₂Me)₂ (2.0 equiv). [d] Time at which reaction was quenched. [e] Determined by ¹³C NMR analysis; *sc* (%) = 100 [(*R_R* – *S_R*)/(*R_R* – *S_R*)] where mol fractions of enantiomeric products (*R_R*-**2** and (*S_R*)-**2** are obtained from (*R*)-**1** (and (*R_S*)-**2** and (*S_S*)-**2**) from (*S*)-**1**. [f] Determined by ¹³C NMR analysis; *ee*_g = global *ee* of overall sample of 1,3-[²H]₁-**2**. [g] Yield of analytically pure 1,3-[²H]₁-**2** obtained after chromatography on silica gel.

neither $\text{Zn}(\text{OAc})_2$ nor CsOAc were effective at activating either pro-catalyst $[(\pi\text{-C}_3\text{H}_5)\text{Pd}(\text{Cl})(P)\text{-4b}]$ or $[(\pi\text{-C}_3\text{H}_5)\text{Pd}(P,C\text{-4b})][\text{O}_3\text{SCF}_3]$ (Table 2, entries 4 and 9); however, a combination of CsOAc (1 mol %) and BSA (2 equiv) did function efficiently (Table 2, entries 1 and 3). Ultimately, LiOMe provided the best catalytic nucleophile system and gave high *sc* and *ee_g* with the carbonate substrates. Overall, it may be noted that although there were no obvious trends within the data set, the highest intrinsic selectivities tend towards those observed with $[\text{NaCH}(\text{CO}_2\text{CH}_3)_2]$.

To further study the effect of NaOAc , we performed stoichiometric reactions which we monitored by ^1H NMR spectroscopy (500 MHz, $[\text{D}_8]\text{THF}/\text{CD}_2\text{Cl}_2$). These experiments revealed that the neutral monodentate complex $[(\pi\text{-C}_3\text{H}_5)\text{Pd}(\text{Cl})(P\text{-4b})]$, generated in situ by reaction of **4b** with $[(\pi\text{-C}_3\text{H}_5)\text{Pd}(\text{Cl})]_2$, fails to react at all with an excess of NaOAc over a period of hours (Scheme 8, lower section). In

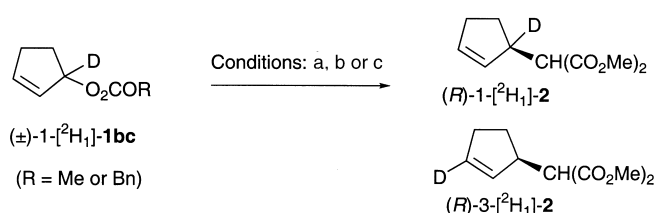


Scheme 8. The generation of ionic bidentate and neutral monodentate MAP–Pd complexes and their relative reactivity towards acetate ion, as monitored by ^1H NMR spectroscopy in $[\text{D}_8]\text{THF}/\text{CD}_2\text{Cl}_2$. When employed in catalytic allylic alkylation, the ready reaction of $[(P,C\text{-4b})\text{-Pd-allyl}]^+$ with MOAc ($\text{M} = \text{Na}, \text{Li}$) provides a useful route to the generation of $[(P,C\text{-4b})\text{-Pd}^0]$ and thus catalytic quantities of malonate anion via the route outlined in the lower section of Scheme 6.

stark contrast, the cationic complex $[(\pi\text{-C}_3\text{H}_5)\text{Pd}(P,C\text{-4b})][\text{O}_3\text{SCF}_3]$ reacts rapidly with one equivalent of NaOAc to yield allyl acetate—as confirmed by reference to independently prepared sample in $[\text{D}_8]\text{THF}/\text{CD}_2\text{Cl}_2$ —and an orange-red Pd co-product which is tentatively assigned as $[(P,C\text{-4b})\text{-Pd}^0]$.^[28] When this reaction mixture was treated with one equivalent of NaCl there was no generation of $[(\pi\text{-C}_3\text{H}_5)\text{Pd}(\text{Cl})(P\text{-4b})]$ from the allyl acetate.

These results highlight the much greater electrophilic reactivity of bidentate cationic allylpalladium complexes of **4b** as compared to the neutral monodentate $\text{Pd}(\text{Cl})$ allyl type complexes. We therefore suggest that under chloride free conditions the initial product of oxidative addition (**5/5'**) $[(\pi\text{-C}_3\text{H}_5)\text{Pd}(P,C\text{-4b})^+][\text{X}]^-$ undergoes ion-pair metathesis with $[\text{M}]^+[\text{CH}(\text{CO}_2\text{Me})_2]^-$ at a rate which is dependent on the identity of the nucleofuge (*X*) and nucleophile counterion (*M*) as well as the nucleophile concentration. These factors

then determine the extent of diastereoisomer equilibration of **5/5'** before nucleophilic attack to give **2** and $[\text{Pd}^0(P,C\text{-4b})]$. If full equilibrium (100% *sc*) has occurred prior to metathesis, this gives **2** in limiting *ee* of about 60% (in THF) irrespective of the identities of '*X*' and '*M*'. In the presence of chloride, irreversible generation of neutral $[(\pi\text{-C}_3\text{H}_5)\text{Pd}(\text{Cl})(P\text{-4b})]$, that is **6/6'** ($\text{Y} = \text{Cl}$) can occur directly^[29] by oxidative addition to $[\text{Pd}(\text{Cl})(P,C\text{-4b})]^-$, or by ion–metathesis (*X* for *Y*) with **5/5'** followed by ion-pair collapse. The effectiveness with which this process can compete depends on the identity of '*X*'. Once generated, reaction with $[\text{MCH}(\text{CO}_2\text{Me})_2]$ gives **2** of lower *ee*, presumably due to the monodentate coordination of **4b**. Thus, even under conditions of catalytic nucleophile generation (2 equiv CH_2E_2 /1 mol % NaOMe), which facilitate high degrees of stereochemical convergence, the *ee_g* values attained with the chloro-bearing pro-catalyst $[(\pi\text{-C}_3\text{H}_5)\text{Pd}(\text{Cl})(P\text{-4b})]$ are significantly lower than those attained with the cationic pro-catalyst (Scheme 9). The significantly lower



Scheme 9. The stark differences in pro-catalyst activation, yield and intrinsic selectivities of chloride (5 mol %) and chloride-free 'Pd-MAP'-systems for the allylic alkylation of cyclopentenyl carbonates **1b/1c** (selected data from Table 1). Conditions: a) 5 mol % $[(\pi\text{-C}_3\text{H}_5)\text{Pd}(\text{Cl})(P\text{-4b})]$, 1 mol % NaOMe , 2 equiv CH_2E_2 , THF, 20 °C, 16 h, 22–30% yield, 84–98% *sc*, 26–44% *ee_g*; b) 5 mol % $[(\pi\text{-C}_3\text{H}_5)\text{Pd}(\text{Cl})(P\text{-4b})]$, 1 mol % NaOAc , 2 equiv CH_2E_2 , THF, 20 °C, 16 h, 0% yield; c) 5 mol % $[(\pi\text{-C}_3\text{H}_5)\text{Pd}(P,C\text{-4b})][\text{OTf}]$, 1 mol % NaOMe or 1 mol % NaOAc , 2 equiv CH_2E_2 , THF, 20 °C, 16 h, 80–89% yield, 95–98% *sc*, 55–59% *ee_g*.

intrinsic selectivity under chloride conditions confirms that reaction of **6/6'** does not occur predominantly by prior ionisation to give the more electrophilic cations **5/5'**.

Conclusion

Comparison of ligands **3** and **4a–c** under standard ("benchmarking") asymmetric Pd-catalysed allylation conditions suggests that **4b** ($(\pm)\text{-1a} \rightarrow 10\% \text{ ee } (R)\text{-2}$) has little potential for the development of a selective alkylation of cyclopentenyl type substrates. However, earlier studies of this reaction have demonstrated that the low selectivity is a result of a powerful memory effect. The factors affecting the memory effect have been studied by analysis of a weighted manipulation of enantiomer ratios, defined as "stereochemical convergence" (*sc*). Graphical analysis of *sc* against global enantiomeric excess (*ee_g*) allows changes in limiting selectivity to be discerned—providing that a simple relationship exists. In this case, whilst the *ee* ultimately attained (ca. 60%) is not spectacular, it can be attained only under *halide-free* conditions and is significantly higher than the *ee* values achieved with ligands **3** and **4c** (8% and 36% respectively). As

suggested earlier,^[4c] the powerful memory effects observed under the standard conditions (e.g. point *i*, Figure 4, graph **I**) arise from selective attack (*trans* to P)^[30] of the primary intermediates **5** and **5'**. In the current case, and unlike conventional Pd-catalysed allylic alkylations in which there is no memory effect, analysis of results from runs in which there is low *sc* indicates that **5a** and **5a'** are attacked with approximately equal regioselectivity (ca. 88 and 80% *trans* to P, respectively) which translates into approximately equal but opposite *ee* values (76 and 60%, respectively). The *ee* value of about 60% obtained at 100% *sc* therefore arises from 88% of the catalytic flux proceeding via attack of **5**, the intermediate generated initially from the matched pairing of substrate and ligand ((*R*)-**1**/(*S*)-**4b**). Using this as the basis for a kinetic model, the relationship between *sc* and *ee_g* can be satisfactorily simulated (see line passing through points in Figure 4, graph **I**). However, it should be noted that assaying the contributions of the equilibrium population and reactivity of **5** and **5'** to the 88% selective flux via **5** is rather challenging since these π -cyclopentenylpalladium intermediates are unstable and thus hard to isolate. Future work will address this issue.

The *sclee* profile obtained in the presence of the palladophilic chloride ion supports the concept that, with ligands **4a** and **4b**, catalyst turnover can proceed via cationic bidentate (*P,C*)-intermediates of type **5** or neutral monodentate (*P*)-intermediates of type **6** depending on the identity of X (or Y).^[31] The latter intermediates induce lower enantioselectivity in the allylic alkylation of cyclopentenyl-type allylic electrophiles, presumably due to the non-chelate nature of the ligand which then exerts less influence on the equilibrium population, relative reactivity and regioselectivity of attack by nucleophile on **6** versus **6'**.

Overall, these results highlight the importance of testing for memory effects and comparing pro-catalysts when testing novel ligands in the benchmark asymmetric Pd-catalysed allylic alkylation reactions. The effect that the commonly employed Pd source [Pd(η^3 -C₃H₅)₂Cl₂] has in the current system, in terms of reactivity, yield and intrinsic selectivity (graphs **I** and **II** in Figure 4; Scheme 9), suggests that comparison of the outcome from a non-halide^[26] bearing pro-catalyst should always be considered.^[32]

Experimental Section

General: Anhydrous solvents (THF, CH₂Cl₂) were obtained by passage through an activated-alumina drying train (Anhydrous Technologies) and reactions were carried out under nitrogen by using standard Schlenk techniques. Allylic substitution reactions (**1** → **2**) were conducted in THF at ambient temperature, under standard conditions^[4c] except as described in the text. Substrates ((\pm)-1-[²H]₂-**1a**^[4b] and (\pm)-1-[²H]₂-**1b**^[4b]), reagents ([NaCH(CO₂Me)₂]^[33]), ligands (**3**,^[34] **4a**,^[13] **4b**,^[14] and **4c**^[35]) and pro-catalysts ([(π -C₃H₅)Pd(*P,C*-**4a**)]₂[O₃SCF₃]^[4c] and [(π -C₃H₅)Pd(*P,C*-**4b**)]₂[O₃SCF₃]^[4c]) were prepared by standard routes, or were a gift (**4c**). NMR experiments were performed on JEOL GX400 and Alpha 500 instruments. Flash column chromatography: Merck silica gel 60; elution with a constant gravity head of about 15 cm solvent. TLC: 0.25 mm, Merck silica gel 60 F254; visualisation at 254 nm or with acidic (H₂SO₄) aqueous KMnO₄ solution (ca. 2%). Yields refer to analytically pure samples obtained after chromatography on silica gel.

Simulation of kinetics and memory effects for simple systems: Kinetics for the idealised reaction (\pm)-**S** → **P** (see inset to Figure 3) via "(+)-**Int** and (–)-**Int**" in which asymmetric induction arises from the combination [*k*_{2,2'} > *k*_{3,3'}; *k*_{–5} > *k*₅] and a memory effect arises from the relationship [*k*_{2,2',3,3'}[Nu] > *k*_{5–5'}], were simulated using MacKinetics.^[36] Using a starting situation of [(\pm)-**S**] = 0.5 [Nu] = 20 [Pd], *k*₁ = 10⁵(*k*_{2,2'}), a large number of models were evaluated, which may be generalised into a) equal, but opposite, stereoselectivity (ranging from 1/3 to 1/10) arising from nucleophilic attack of (+)-**Int** and (–)-**Int**, with variation in *K*₅ b) non-equal, but again opposite, stereoselectivity arising from nucleophilic attack of (+)-**Int** and (–)-**Int** with constant *K* = 0.2 and c) keeping *K*₅ = 1, and varying the relative reactivity of (+)-**Int** versus (–)-**Int** over a scale of 10. In all three cases, *sc* was modulated by varying *k*₅/*k*_{–5} and a double-set of intermediates was generated so that (+)-**S** and (–)-**S** followed non-convergent pathways and thus (+)-**P**₍₊₎, (+)-**P**_(–), (–)-**P**₍₊₎ and (–)-**P**_(–) could be distinguished. The model was allowed to proceed until quantitative conversion of (\pm)-**S** to **P** was predicted.

From the relative concentrations of the components predicted at this point, the global *ee* and *sc* were calculated: *ee_g* = {[(+)-**P**] – [(–)-**P**]} / {[(+)-**P**] + [(–)-**P**]}; *sc* = {[(+)-**P**₍₊₎] – [(–)-**P**_(–)]} / {[(+)-**P**₍₊₎] + [(–)-**P**₍₊₎]} + {[(+)-**P**_(–)] – [(–)-**P**_(–)]} / {[(+)-**P**_(–)] + [(–)-**P**_(–)]}]. These results were plotted on *sc* versus *ee_g* axes (as in Figure 3). In all cases, lines that varied from linear to a smooth convex curve (as in Figure 3) were observed. A more complex model involving generation of *both* intermediates from *both* substrates gave similar results. The models used to calculate the curves passing through points **A** and **B** are as follows: **A**, *k*₁ = 90000; *k*₂ = 9; *k*_{2'} = 5; *k*₃ = 1; *k*_{3'} = 1; *K*₅ = 6. Modulation of *sc* from 16 (min *sc*) to 100 was achieved through *k*_{–5} = 0.00001 → 100000 (for *sc* = 40, *ee_g* = 30, *k*_{–5} = 3.453, *k*₅ = 0.5755); **B**, *k*₁ = 90000; *k*₂ = *k*_{2'} = 9; *k*₃ = *k*_{3'} = 1; *K*₅ = 3. Modulation of *sc* from 0 to 100 was achieved through *k*_{–5} = 0.00001 → 100000 (for *sc* = 60, *ee_g* = 30, *k*_{–5} = 22.38, *k*₅ = 7.46). The model used to calculate the curve through the filled circles in Figure 4, graph **I** is as follows: *k*₁ = 90000; *k*₂ = 8.8; *k*_{2'} = 8.0; *k*₃ = 1.2; *k*_{3'} = 2.0; *K*₅ = 7^{–1}. Modulation of *sc* from 11 (min *sc*) to 100 was achieved through *k*_{–5} = 0.00001 → 100000.

(\pm)-1-[²H]₂-Cyclopent-2-enylbenzylcarbonate ((\pm)-1-[²H]₂-**1c**)^[37] Benzyl chloroformate (1.505 g, 8.82 mmol) in CH₂Cl₂ (2 mL) was added dropwise over 15 min to a stirred solution of (\pm)-1-[²H]₂-cyclopenten-1-ol (0.5 g, 5.88 mmol) in CH₂Cl₂ (7.5 mL) and pyridine (2.5 mL) at 0 °C. The reaction mixture was then stirred for 16 h at 25 °C, poured into water (20 mL) and extracted with CH₂Cl₂ (3 × 50 mL). The combined organic extracts were washed with 1 M hydrochloric acid (2 × 20 mL) and water (2 × 20 mL), dried over MgSO₄ and evaporated under reduced pressure to afford a colourless oil. Purification by column chromatography (2 × 20 cm, elution with hexane/EtOAc, 12:1 v/v) gave (\pm)-1-[²H]₂-**1c** as a colourless oil (1.07 g, 82.9%). *R*_f = 0.41 (hexane/EtOAc 12:1, v/v); ¹H NMR (400 MHz, CDCl₃, 21 °C, Me₄Si): δ = 7.35 (m, 5H; Ar), 6.12 (ddd, ³J(H,H) = 5.6, ^{3,4}J(H,H) = 1.8, 1.8 Hz, 1H; C(3)H), 5.86 (ddd, ³J(H,H) = 5.6, ⁴J(H,H) = 2.0, 2.0 Hz, 1H; C(2)H), 5.11 (s, 2H; PhCH₂), 2.49 (m, 1H; C(4)H_b), 2.26 (m, 2H; C(5)H₂), 1.91 ppm (m, 1H; C(4)H_a); ¹³C{¹H} NMR (100 MHz, CDCl₃, 21 °C, Me₄Si): δ = 167.1 (C=O), 154.84 (C_{ipso}), 138.55 (C(3)H), 128.48 (CH_{arom.}), 128.33 (CH_{arom.}), 128.14 (CH_{arom.}), 121.21 (C(2)H) 83.92 (t, ¹J(C,D) = 23.8 Hz; C(1)D), 69.22 (CH₂Ph), 30.99 (C(5)H₂), 29.46 ppm (C(4)H₂); ²H NMR (46 MHz, CHCl₃, 21 °C, CDCl₃): δ = 5.58 ppm (br. s, 1D; C(1)D); MS (CI): *m/z*: 220 (8) ([MH]⁺), 181 (56), 158 (51), 135 (27), 107 (38), 91 (100), 68 (98).

Palladium-catalysed allylic alkylation with 97% stereochemical convergence: To a stirred mixture of [Pd(η^3 -C₃H₅)(*S*-**4b**)]₂[OTf] (9.8 mg, 0.013 mmol, 5 mol %), under N₂, in degassed dry THF (2 mL) at 25 °C was added (\pm)-1-[²H]₂-**1c** (55.2 mg 0.25 mmol) and dimethylmalonate (66.5 mg, 0.5 mmol, 2 equiv). The reaction was initiated by addition of sodium methoxide (0.1 mg, 25 μ mol, 1 mol %) and then stirred for 1 h, after which time the reaction was complete according to TLC analysis (hexane/EtOAc (12:1 v/v); *R*_f = 0.51 (**1c**)). The reaction mixture was quenched by addition of 10% aqueous NH₄Cl (5 mL) and extracted with CH₂Cl₂ (4 × 5 mL). The combined extracts were dried (MgSO₄) and evaporated under reduced pressure to afford a yellow oil. This oil was taken up in CH₂Cl₂ (1 mL), applied directly to a pre-solvented silica gel column (1 × 20 cm) and eluted with hexane/EtOAc (12:1, v/v), collecting 5 mL fractions (gravity column). Fractions 9 to 14 (containing material of *R*_f = 0.2) were evaporated to afford (*R*)-1,3-[²H]₂-**2** as a colourless oil (50.2 mg, 85%)

with a global *ee* of 59% and 97% *sc*, determined by ^{13}C NMR analysis with (+)-[Eu(hfc)₃] in C₆D₆ as described in ref. [4b].

Acknowledgements

We thank the EPSRC (GR/N05208), GAČR (203/01/D051, 203/00/0601, and 203/00/0632) and Lancaster Synthesis for generous support, NATO for a fellowship (administered by the Royal Society, London) to S.V. and the Royal Society of Chemistry for the Hickinbottom Fellowship (to G.C.L.-J.). Dr John M. Brown FRS, University of Oxford, kindly supplied samples of QUINAP (**4c**), and Dr. Paul J. Wyatt (Bristol) made valuable comments regarding stereochemical nomenclature.

- [1] Reviews: a) G. Consiglio, R. M. Waymouth, *Chem. Rev.* **1989**, *89*, 257–276; b) C. G. Frost, J. Howarth, J. M. J. Williams, *Tetrahedron: Asymmetry* **1992**, *3*, 1089–1122; c) B. M. Trost, D. L. Van Vranken, *Chem. Rev.* **1996**, *96*, 395–422.
- [2] A. Pfaltz, *Acta Chem. Scand.* **1996**, *50*, 189–194, and references therein; b) J. M. Brown, D. I. Hulmes, P. J. Guiry, *Tetrahedron* **1994**, *50*, 4493–4506; c) S. Ramdeehul, P. Dierkes, R. Aguado, P. C. J. Kamer, P. W. N. M. van Leeuwen, J. A. Osborn, *Angew. Chem.* **1998**, *110*, 3302–3304; *Angew. Chem. Int. Ed.* **1998**, *37*, 3118–3121.
- [3] J. C. Fiaud, J. L. Malleron, *Tetrahedron Lett.* **1981**, *22*, 1399–1402.
- [4] For leading references see: a) J. M. Longmire, B. Wang, X. Zhang, *Tetrahedron Lett.* **2000**, *41*, 5435–5439; see also: b) G. C. Lloyd-Jones, S. C. Stephen, *Chem. Eur. J.* **1998**, *4*, 2539–2549; c) G. C. Lloyd-Jones, S. C. Stephen, M. Murray, C. P. Butts, Š. Vyskočil, P. Kočovský, *Chem. Eur. J.* **2000**, *6*, 4348–4357; d) U. Kazmaier, F. L. Zumppe, *Angew. Chem.* **2000**, *112*, 805–807; *Angew. Chem. Int. Ed.* **2000**, *39*, 802–804.
- [5] B. M. Trost, R. C. Bunt, *J. Am. Chem. Soc.* **1996**, *118*, 235–236.
- [6] a) U. Burckhardt, M. Baumann, A. Togni, *Tetrahedron: Asymmetry* **1997**, *8*, 155–159; b) T. Hayashi, M. Kawatsura, Y. Uozumi, *J. Am. Chem. Soc.* **1998**, *120*, 1681–1687.
- [7] I. J. S. Fairlamb, G. C. Lloyd-Jones, *Chem. Commun.* **2000**, 2447–2448.
- [8] G. C. Lloyd-Jones, S. C. Stephen, *Chem. Commun.* **1998**, 2321–2322.
- [9] *Stereospecific*: A reaction in which 'starting materials differing only in their configuration are converted to stereoisomerically distinct products'. *Stereoconvergent*: 'a reaction in which stereoisomerically differing starting materials yield identical products'; E. L. Eliel, S. H. Wilen, L. N. Mander, *Stereochemistry of Organic Compounds*, Wiley Interscience, New York, **1994**.
- [10] Matched refers to a favourable configurational relationship of the substrate with the catalyst. The matched substrate will give an *ee* of product that is closer (or identical) in absolute configuration and magnitude to the intrinsic selectivity of the catalyst as compared to the mismatched. Most often, the matched substrate reacts faster than the mismatched and there will thus be a kinetic resolution process prior to complete reaction.
- [11] For leading references to other ligands that effect high *ee* in this substrate class.^[4a]
- [12] a) P. von Matt, A. Pfaltz, *Angew. Chem.* **1993**, *105*, 614–614; *Angew. Chem. Int. Ed. Engl.* **1993**, *32*, 566–567; b) J. Sprinz, G. Helmchen, *Tetrahedron Lett.* **1993**, *34*, 1769–1772; c) G. J. Dawson, C. G. Frost, J. M. J. Williams, *Tetrahedron Lett.* **1993**, *34*, 3149–3150; d) see also: G. Helmchen, A. Pfaltz, *Acc. Chem. Res.* **2000**, *33*, 336–345.
- [13] T. Hayashi, *Acc. Chem. Res.* **2000**, *33*, 354–362.
- [14] a) Š. Vyskočil, M. Smrčina, V. Hanuš, M. Polášek, P. Kočovský, *J. Org. Chem.* **1998**, *63*, 7738–7748; b) P. Kočovský, Š. Vyskočil, I. Čísařová, J. Sejbál, I. Tišlerová, M. Smrčina, G. C. Lloyd-Jones, S. C. Stephen, C. P. Butts, M. Murray, V. Langer, *J. Am. Chem. Soc.* **1999**, *121*, 7714–7715.
- [15] N. W. Alcock, J. M. Brown, D. I. Hulmes, *Tetrahedron: Asymmetry* **1993**, *4*, 743–756.
- [16] G. C. Lloyd-Jones, *Synlett* **2001**, 161–183.
- [17] Attainment of near-perfect *sc*, for example with (±)-1-[$^2\text{H}_1$]-**1c**, confirms that secondary kinetic isotope effects are small (< 1.05/1.00) in relation to the memory effects that are of interest and thus the results can be translated directly back to the unlabelled substrate.
- [18] C. Amatore, A. Jutand, G. Meyer, L. Mottier, *Chem. Eur. J.* **1999**, *5*, 466–473.
- [19] Note that it has been observed in some cases that diastereoisomer interconversion is accelerated by nucleophile, for example malonate: J. M. Brown, D. I. Hulmes, P. J. Guiry, *Tetrahedron* **1994**, *50*, 4493–4506.
- [20] B. M. Trost, R. C. Bunt, *J. Am. Chem. Soc.* **1998**, *120*, 70–79.
- [21] Fluoride ion added in the form of tetrabutylammonium triphenylsilyldifluoride (TBAT). For preparation see: C. J. Handy, Y.-F. Lam, P. DeShong, *J. Org. Chem.* **2000**, *65*, 3542–3543.
- [22] The recovered 1-[$^2\text{H}_1$]-**1a** had not been scrambled (no 3-[$^2\text{H}_1$]-**1a** was detected by ^1H or ^2H NMR spectroscopy).
- [23] Based on substrate recovered during reaction, there was no evidence for reversibility of ionisation, although this is known with some systems: C. Amatore, S. Gamez, A. Jutand, G. Meyer, M. Moreno-Mañas, L. Morral, R. Pleixats, *Chem. Eur. J.* **2000**, *6*, 3372–3376.
- [24] P. G. Andersson, S. Schab, *Organometallics* **1995**, *14*, 1–2, and references therein.
- [25] Due to the similarity in pK_a of cyclopentadiene with ROH and the ready prototropy in cyclopentadiene, it is hard to conceive of a stereochemical labelling experiment that would confirm either the location or the stereochemistry of the β -elimination.
- [26] For a recent review of some of the effects that halide ions can have on asymmetric transition metal catalysed reactions, including allylic alkylations, see: K. Fagnou, M. Lautens, *Angew. Chem.* **2002**, *114*, 26–49; *Angew. Chem. Int. Ed.* **2002**, *41*, 26–47.
- [27] A. Gogoll, J. Örnebro, H. Grennberg, J.-E. Bäckvall, *J. Am. Chem. Soc.* **1994**, *116*, 3631–3632.
- [28] We were unable to isolate the complex and further manipulation led to decomposition. The partial NMR spectrum for analogous complex [$((P,C)\text{-4a})\text{Pd}^0$] has been reported by Hayashi and co-workers;^[6b] the solid-state structure (single-crystal X-ray diffraction) of a Pd^0 -dba complex of a related phenanthracenyl ligand, displaying P,C -coordination has recently been reported: J. Yin, M. P. Rainka, X.-X. Zhang, S. L. Buchwald, *J. Am. Chem. Soc.* **2002**, *124*, 1162–1163.
- [29] C. Amatore, A. Jutand, *Acc. Chem. Res.* **2000**, *33*, 314–321.
- [30] M. Kollmar, B. Goldfuss, M. Reggelin, F. Rominger, G. Helmchen, *Chem. Eur. J.* **2001**, *7*, 4913–4927, and references therein.
- [31] The relevance of the P,C -coordination mode to catalytic turnover involving ligands of the type $\text{Ar-Ar-PRR}'$, which was first proposed in 1999,^[14b] has recently been challenged: T. Hamada, A. Chieffi, J. Åhman, S. L. Buchwald, *J. Am. Chem. Soc.* **2002**, *124*, 1261–1268.
- [32] For another dramatic effect of chloride in allylic alkylation, see: G. C. Lloyd-Jones, S. C. Stephen, *Chem. Commun.* **1998**, 2321–2322.
- [33] J. M. Brown, J. E. MacIntyre, *J. Chem. Soc. Perkin Trans. 2* **1985**, 961–970.
- [34] C. P. Butts, G. C. Lloyd-Jones, *Tetrahedron* **1998**, *54*, 901–914.
- [35] N. W. Alcock, J. M. Brown, D. I. Hulmes, *Tetrahedron: Asymmetry* **1993**, *4*, 743–756.
- [36] Commercial software (Leipold Associates, USA).
- [37] Unlabelled material: M. T. Powell, A. M. Porte, J. Reibenspies, K. Burgess, *Tetrahedron* **2001**, *57*, 5027–5038.

Received: March 4, 2002 [F3923]